

Observation of a near-threshold enhancement in the $\omega\phi$ mass spectrum from the doubly OZI suppressed decay $J/\psi \rightarrow \gamma\omega\phi$

M. Ablikim¹, J. Z. Bai¹, Y. Ban¹², J. G. Bian¹, X. Cai¹, H. F. Chen¹⁷, H. S. Chen¹, H. X. Chen¹, J. C. Chen¹, Jin Chen¹, Y. B. Chen¹, S. P. Chi², Y. P. Chu¹, X. Z. Cui¹, Y. S. Dai¹⁹, L. Y. Diao⁹, Z. Y. Deng¹, Q. F. Dong¹⁵, S. X. Du¹, J. Fang¹, S. S. Fang², C. D. Fu¹, C. S. Gao¹, Y. N. Gao¹⁵, S. D. Gu¹, Y. T. Gu⁴, Y. N. Guo¹, Y. Q. Guo¹, Z. J. Guo¹⁶, F. A. Harris¹⁶, K. L. He¹, M. He¹³, Y. K. Heng¹, H. M. Hu¹, T. Hu¹, G. S. Huang^{1a}, X. T. Huang¹³, X. B. Ji¹, X. S. Jiang¹, X. Y. Jiang⁵, J. B. Jiao¹³, D. P. Jin¹, S. Jin¹, Yi Jin⁸, Y. F. Lai¹, G. Li², H. B. Li¹, H. H. Li¹, J. Li¹, R. Y. Li¹, S. M. Li¹, W. D. Li¹, W. G. Li¹, X. L. Li¹, X. N. Li¹, X. Q. Li¹¹, Y. L. Li⁴, Y. F. Liang¹⁴, H. B. Liao¹, B. J. Liu¹, C. X. Liu¹, F. Liu⁶, Fang Liu¹, H. H. Liu¹, H. M. Liu¹, J. Liu¹², J. B. Liu¹, J. P. Liu¹⁸, Q. Liu¹, R. G. Liu¹, Z. A. Liu¹, Y. C. Lou⁵, F. Lu¹, G. R. Lu⁵, J. G. Lu¹, C. L. Luo¹⁰, F. C. Ma⁹, H. L. Ma¹, L. L. Ma¹, Q. M. Ma¹, X. B. Ma⁵, Z. P. Mao¹, X. H. Mo¹, J. Nie¹, S. L. Olsen¹⁶, H. P. Peng^{17b}, R. G. Ping¹, N. D. Qi¹, H. Qin¹, J. F. Qiu¹, Z. Y. Ren¹, G. Rong¹, L. Y. Shan¹, L. Shang¹, C. P. Shen¹, D. L. Shen¹, X. Y. Shen¹, H. Y. Sheng¹, H. S. Sun¹, J. F. Sun¹, S. S. Sun¹, Y. Z. Sun¹, Z. J. Sun¹, Z. Q. Tan⁴, X. Tang¹, G. L. Tong¹, G. S. Varner¹⁶, D. Y. Wang¹, L. Wang¹, L. L. Wang¹, L. S. Wang¹, M. Wang¹, P. Wang¹, P. L. Wang¹, W. F. Wang^{1c}, Y. F. Wang¹, Z. Wang¹, Z. Y. Wang¹, Zhe Wang¹, Zheng Wang², C. L. Wei¹, D. H. Wei¹, N. Wu¹, X. M. Xia¹, X. X. Xie¹, G. F. Xu¹, X. P. Xu⁶, Y. Xu¹¹, M. L. Yan¹⁷, H. X. Yang¹, Y. X. Yang³, M. H. Ye², Y. X. Ye¹⁷, Z. Y. Yi¹, G. W. Yu¹, C. Z. Yuan¹, J. M. Yuan¹, Y. Yuan¹, S. L. Zang¹, Y. Zeng⁷, Yu Zeng¹, B. X. Zhang¹, B. Y. Zhang¹, C. C. Zhang¹, D. H. Zhang¹, H. Q. Zhang¹, H. Y. Zhang¹, J. W. Zhang¹, J. Y. Zhang¹, S. H. Zhang¹, X. M. Zhang¹, X. Y. Zhang¹³, Yiyun Zhang¹⁴, Z. P. Zhang¹⁷, D. X. Zhao¹, J. W. Zhao¹, M. G. Zhao¹, P. P. Zhao¹, W. R. Zhao¹, Z. G. Zhao^{1d}, H. Q. Zheng¹², J. P. Zheng¹, Z. P. Zheng¹, L. Zhou¹, N. F. Zhou^{1d}, K. J. Zhu¹, Q. M. Zhu¹, Y. C. Zhu¹, Y. S. Zhu¹, Yingchun Zhu^{1b}, Z. A. Zhu¹, B. A. Zhuang¹, X. A. Zhuang¹, B. S. Zou¹

(BES Collaboration)

¹ *Institute of High Energy Physics, Beijing 100049, People's Republic of China*

² *China Center for Advanced Science and Technology (CCAST), Beijing 100080, People's Republic of China*

³ *Guangxi Normal University, Guilin 541004, People's Republic of China*

⁴ *Guangxi University, Nanning 530004, People's Republic of China*

⁵ *Henan Normal University, Xinxiang 453002, People's Republic of China*

⁶ *Huazhong Normal University, Wuhan 430079, People's Republic of China*

⁷ *Hunan University, Changsha 410082, People's Republic of China*

⁸ *Jinan University, Jinan 250022, People's Republic of China*

⁹ *Liaoning University, Shenyang 110036, People's Republic of China*

¹⁰ *Nanjing Normal University, Nanjing 210097, People's Republic of China*

¹¹ *Nankai University, Tianjin 300071, People's Republic of China*

¹² *Peking University, Beijing 100871, People's Republic of China*

¹³ *Shandong University, Jinan 250100, People's Republic of China*

¹⁴ *Sichuan University, Chengdu 610064, People's Republic of China*

¹⁵ *Tsinghua University, Beijing 100084, People's Republic of China*

¹⁶ *University of Hawaii, Honolulu, HI 96822, USA*

¹⁷ *University of Science and Technology of China, Hefei 230026, People's Republic of China*

¹⁸ *Wuhan University, Wuhan 430072, People's Republic of China*

¹⁹ *Zhejiang University, Hangzhou 310028, People's Republic of China*

^a *Current address: Purdue University, West Lafayette, IN 47907, USA*

^b *Current address: DESY, D-22607, Hamburg, Germany*

^c *Current address: Laboratoire de l'Accélérateur Linéaire, Orsay, F-91898, France*

^d *Current address: University of Michigan, Ann Arbor, MI 48109, USA*

(Dated: October 2, 2018)

An enhancement near threshold is observed in the $\omega\phi$ invariant mass spectrum from the doubly OZI suppressed decays of $J/\psi \rightarrow \gamma\omega\phi$, based on a sample of 5.8×10^7 J/ψ events collected with

the BESII detector. A partial wave analysis shows that this enhancement favors $J^P = 0^+$, and its mass and width are $M = 1812_{-26}^{+19}$ (stat) ± 18 (syst) MeV/ c^2 and $\Gamma = 105 \pm 20$ (stat) ± 28 (syst) MeV/ c^2 . The product branching fraction is determined to be $B(J/\psi \rightarrow \gamma X) \cdot B(X \rightarrow \omega\phi) = (2.61 \pm 0.27$ (stat) ± 0.65 (syst)) $\times 10^{-4}$.

PACS numbers: 12.39.Mk, 13.20.Gd, 13.30.Ce, 14.40.Cs

QCD predicts a rich spectrum of gg glueballs, qqg hybrids and $qq\bar{q}\bar{q}$ four quark states along with the ordinary $q\bar{q}$ mesons in the 1.0 to 2.5 GeV/ c^2 mass region. Radiative J/ψ decays provide an excellent laboratory to search for these states. Until now, no clear experimental signatures for glueballs or hybrids have been found.

Recently, anomalous enhancements near threshold in the invariant mass spectra of $p\bar{p}$ and $p\bar{\Lambda}$ pairs were observed in $J/\psi \rightarrow \gamma p\bar{p}$ [1] and $J/\psi \rightarrow \gamma p\bar{\Lambda}$ [2] decays, respectively, by the BESII experiment. These surprising experimental observations stimulated many theoretical speculations. Therefore it is of special interests to search for possible resonances in other baryon-antibaryon, baryon-meson, and meson-meson final states.

Systems of two vector particles have been intensively studied for signatures of gluonic bound states. Pseudoscalar enhancements in $\rho\rho$ and $\omega\omega$ final states have been seen in radiative J/ψ decays [3, 4, 5, 6], and resonant $\phi\phi$ structures have also been observed near threshold in πp scattering experiments [7]. The radiative J/ψ decay $J/\psi \rightarrow \gamma\omega\phi$ is a doubly OZI suppressed process, and its production ratio should be suppressed by at least one order of magnitude. Therefore, the measurement of this decay and the search for possible resonant states will provide useful information on two vector meson systems. MARKIII collaboration [8] studied $J/\psi \rightarrow \gamma\omega\phi$ decays, but did not find clear structures in the $\omega\phi$ invariant mass spectrum. The final states of $\omega\phi$ were also observed in photon-photon collisions by ARGUS [9, 10] experiment and the cross sections were measured [10].

In this letter, we report on the measurement of the doubly OZI suppressed $J/\psi \rightarrow \gamma\omega\phi$ decay and an enhancement near threshold in the $\omega\phi$ invariant mass spectrum, using 5.8×10^7 J/ψ events collected with the upgraded Beijing Spectrometer (BESII) at the Beijing Electron-Positron Collider (BEPC). BESII is a large solid-angle magnetic spectrometer that is described in detail in Ref. [11].

The $J/\psi \rightarrow \gamma\omega\phi$ ($\omega \rightarrow \pi^+\pi^-\pi^0$, $\phi \rightarrow K^+K^-$) candidate events are required to have four charged tracks, each of which is well fitted to a helix that is within the polar angle region $|\cos\theta| < 0.8$ in the main drift chamber (MDC) and has a transverse momentum larger than 50 MeV/ c . The total charge of the four tracks is required to be zero. For each track, the time-of-flight (TOF) and specific ionization (dE/dx) measurements in MDC are combined to form particle identification Chi-squares for the π , K, and p hypotheses, and the overall Chi-square is determined by adding those of the individual tracks.

The $K^+K^-\pi^+\pi^-$ combination is chosen as the combination with the smallest combined particle identification Chi-square, $\chi^2(\pi^+\pi^-K^+K^-)$, which is required to be smaller than $\chi^2(\pi^+\pi^-\pi^+\pi^-)$ (for the $\pi^+\pi^-\pi^+\pi^-$ hypothesis) and $\chi^2(K^+K^-K^+K^-)$ (for the $K^+K^-K^+K^-$ hypothesis) to remove the background with $\pi^+\pi^-\pi^+\pi^-$ and $K^+K^-K^+K^-$ final states.

Candidate photons are required to have an energy deposit in the barrel shower counter (BSC) greater than 40 MeV, to be isolated from charged tracks by more than 10° , and to have the difference of angle between the cluster development direction in the BSC and the photon emission direction less than 60° . The number of photons is required to be in the range from 3 to 6.

A five-constraint (5C) energy-momentum conservation kinematic fit is made under the $J/\psi \rightarrow \gamma K^+K^-\pi^+\pi^-\pi^0$ hypothesis with the invariant mass of the $\gamma\gamma$ pair associated with the π^0 being constrained to m_{π^0} . The combination of gammas with the largest probability is chosen as the best combination, and events with probability larger than 1% are retained.

To remove backgrounds from $J/\psi \rightarrow K^+K^-\pi^+\pi^-\pi^0$ and $J/\psi \rightarrow K^+K^-\pi^+\pi^-\pi^0\pi^0$, a 5C kinematic fit to the $J/\psi \rightarrow K^+K^-\pi^+\pi^-\pi^0$ hypothesis and a 6C kinematic fit to $J/\psi \rightarrow K^+K^-\pi^+\pi^-\pi^0\pi^0$ (if the number of good photons is greater than 4) are performed, and the probabilities are required to be less than that from the 5C fit to the signal channel. To remove background where the π^0 is falsely reconstructed from a high energy photon and a second spurious shower, the requirement $|E_{\gamma 1} - E_{\gamma 2}|/|E_{\gamma 1} + E_{\gamma 2}| < 0.90$ is applied to the photons forming the π^0 . Here, $E_{\gamma 1}$ and $E_{\gamma 2}$ are the energies of the two photons.

Fig. 1(a) shows the scatter plot of the $m_{K^+K^-}$ versus the $m_{\pi^+\pi^-\pi^0}$ invariant mass after applying the above selection criteria. Two clusters are clearly seen, which indicate the direct observation of the decays of $J/\psi \rightarrow \gamma\omega\phi$ and $\gamma\phi\phi$. The K^+K^- invariant mass distribution is shown in Fig. 1(b), where the ϕ signal can be seen clearly. The $\pi^+\pi^-\pi^0$ invariant mass distribution of candidate events with $m_{K^+K^-}$ in the ϕ range ($|m_{K^+K^-} - m_\phi| < 15$ MeV/ c^2) is shown as the open histogram in Fig. 1(c), where ω and ϕ signals are seen. The shaded histogram in Fig. 1(c) is the $\pi^+\pi^-\pi^0$ invariant mass spectrum recoiling against the ϕ sideband region (15 MeV/ $c^2 < |m_{K^+K^-} - m_\phi| < 30$ MeV/ c^2), where, only a very small ω signal is observed which comes from backgrounds such as $J/\psi \rightarrow \omega K^+K^-$, ωK^*K^- , etc. Since the decays of $J/\psi \rightarrow \omega\phi$ and $\pi^0\omega\phi$ are forbidden by C-

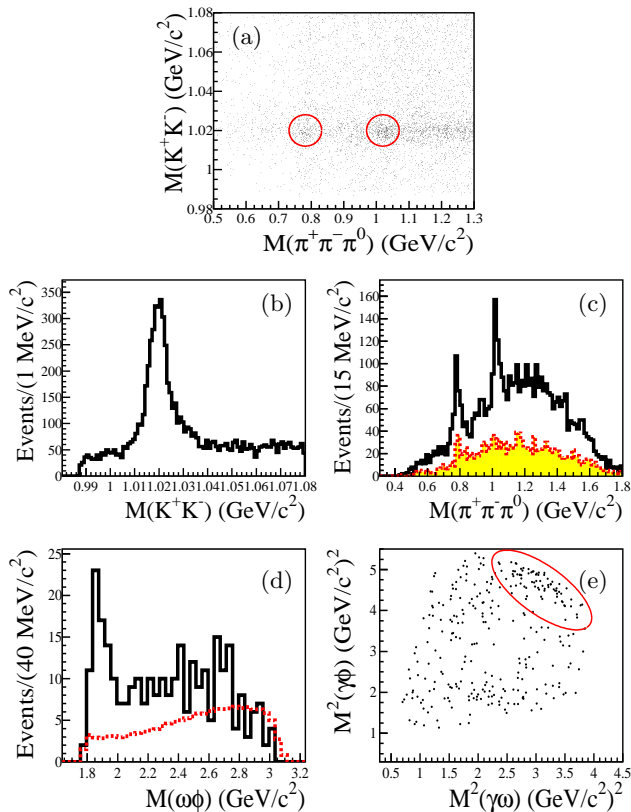


FIG. 1: (a) The scatter plot of the $m_{K^+K^-}$ versus the $\pi^+\pi^-\pi^0$ invariant mass. (b) The K^+K^- invariant mass distribution. (c) The $\pi^+\pi^-\pi^0$ invariant mass distribution; the open histogram is for candidate events with $m_{K^+K^-}$ being in the ϕ range, and the shaded histogram is for events with $m_{K^+K^-}$ being in the ϕ sideband region. (d) The $K^+K^-\pi^+\pi^-\pi^0$ invariant mass distribution for the $J/\psi \rightarrow \gamma\omega\phi$ candidate events. The dashed curve indicates the acceptance varying with the $\omega\phi$ invariant mass. (e) Dalitz plot.

invariance, the 294 observed $\omega\phi$ events present direct evidence for the radiative $J/\psi \rightarrow \gamma\omega\phi$ decay.

The histogram in Fig. 1(d) shows the $K^+K^-\pi^+\pi^-\pi^0$ invariant mass distribution for events with K^+K^- invariant mass within the nominal ϕ mass range ($|m_{K^+K^-} - m_\phi| < 15 \text{ MeV}/c^2$) and the $\pi^+\pi^-\pi^0$ mass within the ω mass range ($|m_{\pi^+\pi^-\pi^0} - m_\omega| < 30 \text{ MeV}/c^2$), and a structure peaked near $\omega\phi$ threshold is observed. There is no evidence of an η_c signal in the $\omega\phi$ invariant mass spectrum. The dashed curve in the figure indicates how the acceptance varies with invariant mass. The acceptance decreases as the invariant mass of $\omega\phi$ becomes smaller due to the decay of the kaon. The peak is also evident as a diagonal band along the upper right-hand edge of the Dalitz plot in Fig. 1(e). There is also a horizontal band near $m_{\gamma K^+K^-}^2 = 2 \text{ (GeV}/c^2)^2$ in the Dalitz plot, which mainly comes from background due to $J/\psi \rightarrow \omega K^* K$.

To ensure that the structure at the $\omega\phi$ mass threshold is not due to background, we have studied potential

background sources using both data and Monte Carlo (MC) data. Non- ω and non- ϕ background are studied using ω and ϕ sideband events. Fig. 2(a) shows the $K^+K^-\pi^+\pi^-\pi^0$ invariant mass of events within the ω sideband ($50 \text{ MeV}/c^2 < |m_{\pi^+\pi^-\pi^0} - m_\omega| < 80 \text{ MeV}/c^2$, $|m_{K^+K^-} - m_\phi| < 15 \text{ MeV}/c^2$), Fig. 2(b) shows the corresponding spectrum of events within the ϕ sideband ($|m_{\pi^+\pi^-\pi^0} - m_\omega| < 30 \text{ MeV}/c^2$, $15 \text{ MeV}/c^2 < |m_{K^+K^-} - m_\phi| < 30 \text{ MeV}/c^2$), and Fig. 2(c) shows the events in the corner region, which is defined as ($50 \text{ MeV}/c^2 < |m_{\pi^+\pi^-\pi^0} - m_\omega| < 80 \text{ MeV}/c^2$, $15 \text{ MeV}/c^2 < |m_{K^+K^-} - m_\phi| < 30 \text{ MeV}/c^2$). The background is estimated by summing up the normalized backgrounds in Fig. 2(a) and Fig. 2(b) and subtracting that in Fig. 2(c), and it is shown as the shaded histogram in Fig. 2(d). No evidence of an enhancement near $\omega\phi$ threshold is observed from the non- ω and non- ϕ background events.

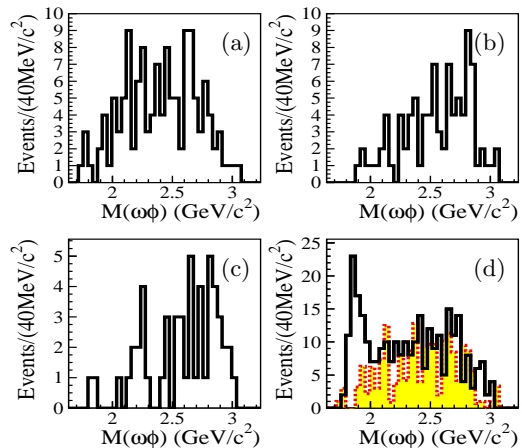


FIG. 2: The $K^+K^-\pi^+\pi^-\pi^0$ invariant mass distribution for (a) the events in the ω sideband; (b) the events in the ϕ sideband; (c) the events in the corner region; (d) for events in the $\omega\phi$ range, as described in the text. The shaded histogram in (d) represents the background distribution obtained from the sideband evaluation.

Exclusive MC samples of J/ψ decays which have similar final states are generated to check whether a peak near $\omega\phi$ mass threshold can be produced. The main backgrounds come from $J/\psi \rightarrow \omega K^* K$, $K^* \rightarrow K\pi^0$. About 45 ± 17 $J/\psi \rightarrow \omega K^* K$, $K^* \rightarrow K\pi^0$ events remain in the $\omega\phi$ invariant mass. However, they peak at the high mass region and do not produce a peak near the threshold. We also checked possible backgrounds with a 60 million Monte-Carlo $J/\psi \rightarrow \text{anything}$ sample, generated by the LUND-Charm model [12]. None of the MC channels produces a peak near threshold in the $\omega\phi$ invariant mass spectrum. In addition, the data taken at the e^+e^- center of mass energy of 3.07 GeV , with a luminosity of $2272.8 \pm 36.4 \text{ nb}^{-1}$ are used to check the continuum contribution. No events are survived. As a check, the measurement of the branching fraction of $J/\psi \rightarrow \gamma\phi\phi \rightarrow$

$\gamma\pi^+\pi^-\pi^0K^+K^-$ is performed, and the result is consistent with that from $J/\psi \rightarrow \gamma\phi\phi \rightarrow \gamma K^+K^-K^+K^-$, but with a larger error.

A partial wave analysis is used to study the spin-parity of the enhancement, denoted as X . The amplitudes are constructed with the covariant helicity coupling amplitude method [13], and the maximum likelihood method is utilized. The decay process is described with sequential 2-body or 3-body decays: $J/\psi \rightarrow \gamma X$, $X \rightarrow \omega\phi$, $\omega \rightarrow \pi^+\pi^-\pi^0$, and $\phi \rightarrow K^+K^-$. The resonance X is parameterized by a Breit-Wigner with constant width, and the background is approximated by non-interfering phase space. The ω decay amplitude is not considered in the fit. The details of the likelihood function construction can be seen in Ref. [14].

When $J/\psi \rightarrow \gamma X$, $X \rightarrow \omega\phi$ is fitted with both the $\omega\phi$ and γX systems being \mathcal{S} -wave, which corresponds to a $X = 0^{++}$ scalar state considering the C-parity of the $\omega\phi$ system, the fit gives the best log likelihood value of -79.55. The fit gives 95 ± 10 events with mass $M = 1812_{-26}^{+19}$ MeV/ c^2 , width $\Gamma = 105 \pm 20$ MeV/ c^2 , and a statistical significance larger than 10σ . Fig. 3(a) shows the comparison of the $\omega\phi$ invariant mass distributions between data and MC projection with the fitted parameters. The comparisons of the angular distributions between data and MC projection for the events with the invariant mass less than 2.0 GeV/ c^2 are shown in Fig. 3(b) - (f).

If the decay of the γX system in $J/\psi \rightarrow \gamma X$, $X \rightarrow \omega\phi$ is treated as \mathcal{D} -wave or a combination of both \mathcal{D} and \mathcal{S} -wave, the mass and width of the X , as well as the log likelihood value do not change much. However, if the decay of the X to $\omega\phi$ is fitted with a \mathcal{D} -wave, the log likelihood value gets worse by about 40. This means that the orbital angular momentum of the $X \rightarrow \omega\phi$ decay can be well separated between \mathcal{S} -wave and \mathcal{D} -wave, while it is difficult to determine in the γX system. A fit with \mathcal{P} -wave decays in both the $\omega\phi$ system and γX systems, corresponding to X being a 0^{-+} pseudoscalar state, makes the log likelihood value worse by 58. Theoretically, the 0^{-+} hypothesis can be well separated from the 0^{++} hypothesis by the distributions of the polar angle of the K^+ (θ_{K^+}) in the ϕ rest system, the polar angle of the normal to the ω decay plane (θ_ω) in the ω rest system, and χ , the angle between the azimuthal angles of the normal to the ω decay plane and the momentum of a K from ϕ decay in the X rest system. We also tried to fit the resonance X with 2^{++} and 2^{-+} spin-parity hypotheses with all possible combinations of orbital angular momenta in the $\omega\phi$ and γX systems. The log likelihood values of the best fits are $-\text{Log}(\mathcal{L}) = -74.80$ and $-\text{Log}(\mathcal{L}) = -63.81$ for 2^{++} and 2^{-+} assignments, respectively. Although the fit is not too much worse for the 2^{++} case, there is only one free parameter for 0^{++} , while there are four free parameters for 2^{++} . Also for 2^{++} , \mathcal{D} -wave is required in $X \rightarrow \omega\phi$; if only \mathcal{S} -wave is used in the fit,

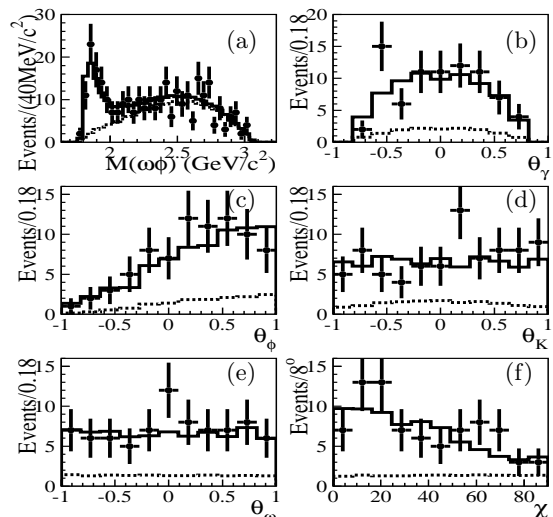


FIG. 3: Comparison between data and MC projections using the fitted parameters for the $\omega\phi$ invariant mass distribution and the angular distributions for the events with $\omega\phi$ invariant mass less than 2.0 GeV/ c^2 . Points with error bars are data, the solid histogram is the MC projection, and the dashed line is the background contribution. (a) The $\omega\phi$ invariant mass distribution; (b) The polar angle of radiative photon (θ_γ); (c) The polar angle of the ϕ in the $\omega\phi$ rest system (θ_ϕ). (d) The polar angle of kaon in the ϕ rest system (θ_K) (e) The polar angle of the normal to the ω decay plane in the ω system. (θ_ω) (f) The χ distribution - the angle between azimuthal angles of the normal to the ω decay plane and the momentum of a kaon from ϕ decay in the X rest system.

$-\text{Log}(\mathcal{L}) = -67$, which is much worse than the final fit. Therefore we conclude that the J^{PC} of the enhancement X favors 0^{++} .

Using the selection efficiency of 1.44%, determined from Monte-Carlo simulation, we obtain the product of the branching fractions as:

$$\mathcal{B}(J/\psi \rightarrow \gamma X) \cdot \mathcal{B}(X \rightarrow \omega\phi) = (2.61 \pm 0.27) \times 10^{-4}.$$

Since phase space $J/\psi \rightarrow \gamma\omega\phi$ decays exist, fitting with an interfering phase space (0^+) is also performed, and the differences between fitting with non-interfering phase space for the mass, width, and branching ratio are 0.5%, 21.9% and 13.8%, respectively. The differences will be included as systematic errors.

The systematic uncertainties on the mass and width come from the uncertainties in the background, the mass calibration, and the interference with phase space, as well as possible biases due to the fitting procedure. The latter are estimated from differences between the input and output masses and widths from MC samples, which are generated as $J/\psi \rightarrow \gamma 0^{++}, 0^{++} \rightarrow \omega\phi$ with \mathcal{S} -wave in both the $\omega\phi$ and γX systems. The uncertainties in the background include the uncertainty in the amount of background as well as the treatment of the background in the fitting. We also tried to subtract the background

determined from the sidebands in the fit instead of using the non-interfering or interfering phase space background, and the differences are taken as systematic errors. The total systematic errors on the mass and width are determined to be $18 \text{ MeV}/c^2$ and $28 \text{ MeV}/c^2$, respectively. The systematic errors in the branching fraction measurement mainly come from the efficiency differences between the Monte-Carlo simulation and data, which include the systematic uncertainties of the tracking efficiency, the photon detection efficiency, the particle identification efficiency, the kinematic fit, and the ω and ϕ decay branching fractions, the amount of background, MC statistics, the fitting procedures, different treatment of background, and the total number of J/ψ events. The total relative systematic error on the product branching fraction is 25%.

In summary, the doubly OZI suppressed decay of $J/\psi \rightarrow \gamma\omega\phi, \omega \rightarrow \pi^+\pi^-\pi^0, \phi \rightarrow K^+K^-$ is studied. An enhancement near $\omega\phi$ threshold is observed with a statistical significance of more than 10σ . From a partial wave analysis with covariant helicity coupling amplitudes, the spin-parity of the $X = 0^{++}$ with an \mathcal{S} -wave $\omega\phi$ system is favored. The mass and width of the enhancement are determined to be $M = 1812_{-26}^{+19}$ (stat) ± 18 (syst) MeV/c^2 and $\Gamma = 105 \pm 20$ (stat) ± 28 (syst) MeV/c^2 , and the product branching fraction is $\mathcal{B}(J/\psi \rightarrow \gamma X) \cdot \mathcal{B}(X \rightarrow \omega\phi) = (2.61 \pm 0.27 \text{ (stat)} \pm 0.65 \text{ (syst)}) \times 10^{-4}$. The mass and width of this state are not compatible with any known scalars listed in the Particle Data Group (PDG) [15]. It could be an unconventional state [16, 17, 18, 19, 20]. However, more statistics and further studies are needed to clarify this.

The BES collaboration thanks the staff of BEPC and computing center for their hard efforts. This work is supported in part by the National Natural Science Foundation of China under contracts Nos. 10491300, 10225524, 10225525, 10425523, 10521003, the Chinese Academy of

Sciences under contract No. KJ 95T-03, the 100 Talents Program of CAS under Contract Nos. U-11, U-24, U-25, and the Knowledge Innovation Project of CAS under Contract Nos. KJCX2-SW-N10, U-602, U-34 (IHEP), the National Natural Science Foundation of China under Contract No. 10225522 (Tsinghua University), and the Department of Energy under Contract No. DE-FG02-04ER41291 (U Hawaii).

-
- [1] J. Z. Bai et al. (BES Collaboration), Phys. Rev. Lett. 91, 022001 (2003).
 - [2] M. Ablikim et al. (BES Collaboration), Phys. Rev. Lett. 93, 112002 (2004).
 - [3] R. M. Baltrusaitis et al., Phys. Rev. D 33, 1222 (1982).
 - [4] D. Bisello et al., Phys. Rev. D 39, 701 (1989).
 - [5] R. M. Baltrusaitis et al., Phys. Rev. Lett 55, 1723 (1985).
 - [6] D. Bisello et al., Phys. Lett. B 192, 239 (1987).
 - [7] A. Etkin et al., Phys. Rev. Lett. 49, 1620 (1982).
 - [8] J. Becker et al., SLAC-PUB-4242, Feb 1987. 10pp. Contributed to 23rd Int. Conf. on High Energy Physics, Berkeley, CA, Jul 16-23, 1986.
 - [9] H. Albrecht et al., Phys. Lett. B 210, 273 (1988).
 - [10] H. Albrecht et al., Phys. Lett. B 332, 451, (1994).
 - [11] J. Z. Bai et al. (BES Collaboration), Nucl. Instr. Meth. A344, 319 (1994).
 - [12] J. C. Chen et al., Phys. Rev. D 62, 034003 (2000).
 - [13] N. Wu and T. N. Ruan, Commun. Theor. Phys. (Beijing, China) 35, 547 (2001) and 37, 309 (2002).
 - [14] M. Ablikim et al. (BES Collaboration), Phys. Rev. D 72, 092002 (2005).
 - [15] Particle Data Group, S. Eidelman et al., Phys. Lett. B592, 1 (2004).
 - [16] Bing An Li, hep-ph/0602072
 - [17] Xiao-Gang He, Xue-Qian Li et al., Phys. Rev. D 73, 051502 (2006).
 - [18] Pedro Bicudo et al., hep-ph/0602172
 - [19] Kuang-Ta Chao, hep-ph/0602190
 - [20] D.V. Bugg, hep-ph/0603018